Comparative Divertor-Transport Study for Helical Devices

Y. Feng 1), M. Kobayashi 2), F. Sardei 1), S. Masuzaki 2), J. Kisslinger 1), T. Morisaki 2), P. Grigull 1), H. Yamada 2), K. McCormick 1), N. Ohyabu 2), R. König 1), I. Yamada 2), L. Giannone 1), K. Narihara 2), U. Wenzel 1), S. Morita 2), H. Thomsen 1), J. Miyazawa 2), N. Ramasubramanian 1), T. Watanabe 2), N. Ashikawa 2), K. Ida 2), A. Komori 2), O. Motojima 2), Y. Nakamura 2), B.J. Peterson 2), K. Sato 2), M. Shoji 1), N. Tamura 2), M. Tokitani 2), the LHD experimental group 2)

1) Max-Planck-Institut für Plasmaphysik, Euratom Association, Germany
2) National Institute for Fusion Science, Toki, Japan

email: feng@ipp.mpg.de

Abstract. Using the island divertors (ID) of W7-AS and W7-X and the helical divertor (HD) of LHD as examples, the paper presents a comparative divertor transport study for three typical helical devices of different machine-size following two distinct divertor concepts, aiming at identifying common physics issues/effects for mutual validation and combined studies. Based on EMC3/EIRENE simulations supported by experimental results, the paper first reviews and compares the essential transport features of the W7-AS ID and the LHD HD in order to build a base and framework for a predictive study of W7-X. Revealed is the fundamental role of the low-order magnetic islands in both divertor concepts. Preliminary EMC3/EIRENE simulation results for W7-X are presented and discussed with respect to W7-AS and LHD in order to show how the individual field and divertor topologies affect the divertor transport and performance. For instance, a high recycling regime which is absent from W7-AS and LHD is expected for W7-X. Topics addressed are restricted to the basic function elements of a divertor such as particle flux enhancement and impurity retention. In particular, the divertor function on reducing the influx of intrinsic impurities is examined for all the three devices under different divertor plasma conditions. Special attention is paid to examining the island screening potential of intrinsic impurities which has been predicted for all the three devices under high divertor collisionality conditions. The results are discussed in conjunction with the experimental observations for high density divertor plasmas in W7-AS and LHD.

1. Introduction

Unlike the standard poloidal-field divertor in tokamaks, divertor concepts presently investigated in stellarators are based on specific edge magnetic field structures intrinsically available in each device [1]. Typical examples are the island divertor (ID) for the advanced low-shear stellarators W7-AS [2] and W7-X [3], and the helical divertor (HD) for the high-shear, largest heliotron-type device LHD [4]. The large existing differences in machine type and size, in combination with the inherent high configutional flexibility of each helical device, open a broad configuration spectrum for exploring divertor solutions for plasma exhaust in helical devices, introducing however, besides the inherent three-dimensionality, another additional independent parameter, i.e. the divertor configuration, in studying the divertor physics within the stellarator community. Inter-machine comparisons are important not only for revealing the configurational dependence of divertor functionality and performance but also for identifying common interesting physics effects for mutual validation and combined studies. For this, the EMC3/EIRENE code [5, 6] provides a useful interpretative and predictive tool. On the other hand, an enriched divertor database contributed from different machines provides a broader basis for code validation to improve the code prediction capability for next-step devices.

Comparison between the W7-AS ID and the LHD HD has been made for specific topics. On an experimental basis, the essential detachment behaviour in LHD has been compared with that in W7-AS, showing that sustained detachment can be achieved in both devices, with the detached plasmas, however, evolving through different paths to different states [7]. Using the

W7-AS ID as reference, the momentum transport in the HD of LHD has been studied using the EMC3/EIRENE code in comparison with experimental results [8], concluding that the suppression of a high recycling regime in LHD is due to a geometric momentum loss process similar to that claimed for W7-AS [9]. This finding has triggered detailed studies to find the common geometric elements governing the SOL transport in both devices, having identified the fundamental role of the low-order islands in both divertor concepts [10]. From this starting point, the island screening potential of intrinsic impurities, which is shown by EMC3/EIRENE simulations for the ID of W7-AS under high SOL collisionalities [11], was also examined and found for the HD of LHD [12]. The numerical results are consistent with the experimental observations of the drop of Fe-line radiation in high density divertor plasmas in both devices [13, 14]. A direct support has been recently provided by the edge spectroscopic measurements on LHD, which show, with increasing the plasma density, a relative shift of carbon line emission from high to low charge states populated in different SOL depths [15].

The first-step results from the joint-studies between W7-AS and LHD are promising, encouraging a predictive study for W7-X. The paper presents the first EMC3/EIRENE simulation results for the ID of W7-X and compares the essential divertor transport features of three typical helical devices of different size and geometry.

2. Divertor concept and geometry

W7-AS and W7-X are low-shear stellarators having a five-fold field symmetry. The low-shear in the Wendelstein-7 series allows large island formation as the radial size of the islands scales as $r_i \propto \sqrt{Rb_{mn}/m\iota'}$ where R is major radius, b_{mn} the resonant radial perturbation field normalized to the toroidal field, m the poloidal mode number and ι´ the shear. Within the respective ι-ranges available in each device, a number of low-order islands with different poloidal mode numbers are suitable for the ID. The so-called standard ID configurations for W7-AS and W7-X are based on the 5/9 and 5/5 island chains, respectively, as shown in Figure 1. That particles and energy entering the islands across the inner separatrix are guided by the open field lines inside the islands towards the targets positioned at the outer separatrix over an appropriate distance away from the confinement core is the functional principle of the ID concept. The island size and the internal field-line pitch, which influence the island divertor transport, can be adjusted externally by ten control coils installed on each machine.

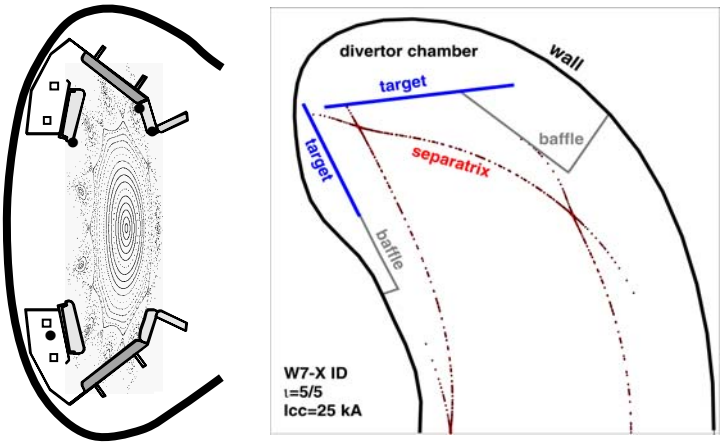

Fig.1 Standard island divertor configurations for W7-AS (left) and W7-X (right, only a half) with respective nine and five islands at the edge. The two devices follow the same ID concept, equipped with similar divertor modules shaped and positioned according to the machine symmetry.

LHD is the largest heliotron-type device with 10 field periods and has a large shear, especially at the edge. The rotational transform in the edge region of the HD configurations covers countless resonances which overlap each other, forming a stochastic layer of ~10 cm thickness. Unlike the single island chains in W7-AS and W7-X, the stochastic SOL in LHD exhibits a complex field structure characterized by coexistence of remnant magnetic islands,

stochastic fields and edge surface layers. In the outermost region close to the wall, the increased poloidal field components of the two helical coils create 4 divertor legs which are cut by graphite targets positioned just in front of the wall (figure 2), forming a divertor configuration similar to the double-null configuration in tokamaks. However, the resulting short connection lengths between the 'X'-points and the targets, which take ~2 m on average, make the divertor legs transparent for the recycling neutrals, at least for the present open divertor configuration [8]. Thus, in the following, we pay our attention only to the stochastic layer.

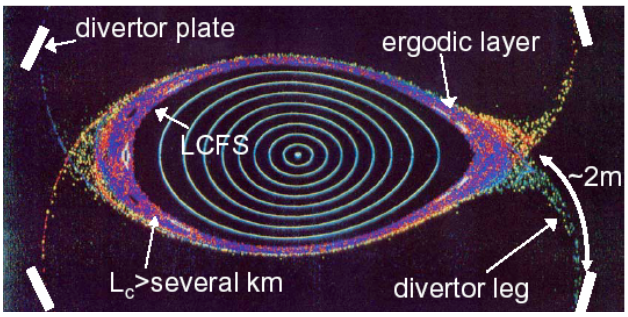

Fig. 2 Field and divertor geometry of the helical divertor in LHD.

The divertor-relevant geometric parameters for the respective standard ID configurations in W7-AS and W7-X are listed in Table 1, where the last four parameters have only a representative meaning because of the complex 3D SOL structures. The field line pitch Θ, which defines the relative perpendicular displacement of a field line towards the targets per field-line length, is estimated for the divertor regions by measuring the parallel and perpendicular X-point-to-target distances $L_{c,x\text{-}t}$ (connection length of the X-point) and Δx, i.e. $\Theta = \Delta x / L_{c,x\text{-}t}$. LHD has a major radius of *3.9 m* and a minor radius of *0.6 m*. The rotational transform in the stochastic layer varies from ~10/7 to 10/2. The open field lines in the stochastic layer exhibit a rather complex evolution structure, yielding a connection length contour ranging from several m to several km. The outermost region is dominated by field lines of short connection lengths. There exist, however, multiple edge surfaces [4] filled by long field lines of several 100 m connection length, forming the main plasma transport channels through the stochastic layer. Thus, the characteristic perpendicular-to-parallel transport scale-length ratio in LHD, i.e. the 10 cm SOL thick divided by several 100 m connection length, is even smaller than those in the IDs of W7-AS and W7-X.

Table 1: Comparison of island-divertor-relevant geometric parameters between W7-AS and W7-X.
L_c=target-target connection length, Δx=target-core distance, Δy = poloidal island width, Θ = pitch

	R (m)	a (m)	ι	L_c (m)	Δx(cm)	Δy(cm)	Θ (10^{-3})
W7-AS	2.0	0.14	5/9	~100	~4	~10	~1-1.5
W7-X	5.5	0.50	5/5	~180	~7-8	~ 60	~2-3

3. Role of low-order magnetic islands

Plasma transport in the island SOL of W7-AS can well be explained in terms of regular magnetic islands [9]. In contrast, Poincare plots indicate a stochastic behavior of the field lines in the HD SOL of LHD. In order to clarify to what extent the plasma as fluid follows the complex field structure in LHD, EMC3/EIRENE simulations have been performed [10]. The following transport analysis is based on a vacuum configuration with R = 3.75 m. The lower picture of figure 3 shows the field line connection length contour together with Poincare plots on the ϕ-position of Thomson measurements. The SOL begins with the 10/7 island chain in which the field lines in the most region become irregular, with small island cores remaining. A similar situation is also presented by the 10/6 island chain. Moving outwards, closed island cores vanish and Poincare-plots show a strong irregularity of the field lines, thus indicating

that the field is stochastic. On the other hand, the underlying connection length contour shows a strong field-line correlation even in the outer region without remnant island cores. The connection length contour reflects actually the basic field structure of low-order resonances. Indeed, all the low-order modes expected within the give ι-range can be identified [10]. The upper picture of figure 3 shows the calculated and Thomson-scattering T_e-profiles along the inboard midplane. Both the code and Thomson results show clearly the impact of the low-order 10/7, 10/5 and 10/3 magnetic islands on electron energy transport. The 10/8, 10/6 and 10/4 mode structures have a poloidally-shifted phase distribution, with the X-points being on the midplane. This is the reason why they are not reflected by the T_e-profiles. In addition, the code shows a strong correlation of parallel plasma flows with the island structure where positive and negative flows surround the O-points [10]. Even for the mode structures without a closed island core, flow channels residing on the island chains are still identifiable. Thus, it is to conclude that the plasma transport in the stochastic layer is governed by the low-order islands, although the relative importance of the stochastic effects can not yet be quantified.

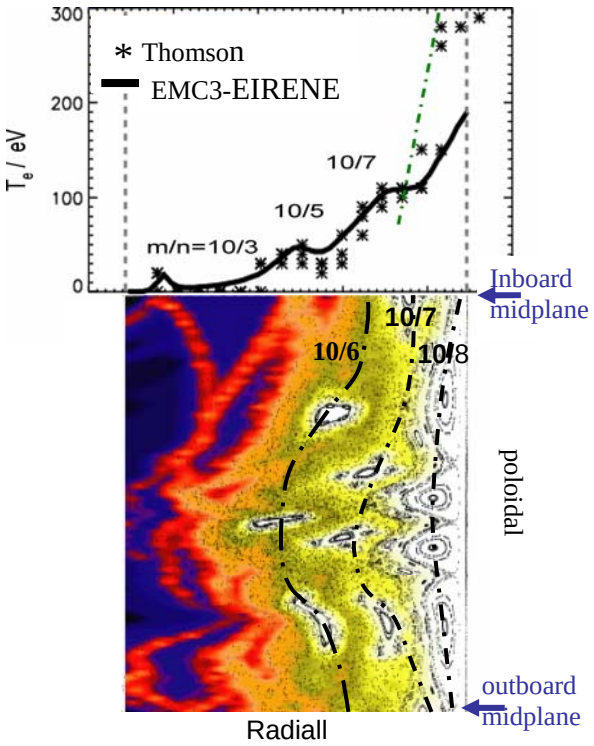

Fig.3 Comparison of Te-profiles between simulations and Thomson measurements (top) and a radially-zoomed connection length contour with an overlying Poincare plot (bottom) over half poloidal field period at a toroidal location where the long axis of the elliptical cross-section lies horizontally. The three dot-dashed lines indicate the 10/6, 10/7 and 10/8 island chains which have remnant closed island cores.

4. Transport characteristics

In the context of fluid approximation, particle transport along field lines is governed by a classical convective process, with the parallel flow velocity being determined by momentum balance. Momentum transport in both W7-AS and LHD divertor configurations is characterized by friction between opposite flows in different parts of the magnetic islands, which gives rise to significant momentum loss and thereby breaks up the pressure conservation along open field lines already under low-density, high-temperature conditions without intensive plasma-neutral interaction. In W7-AS, interaction between opposite flows occurs in both

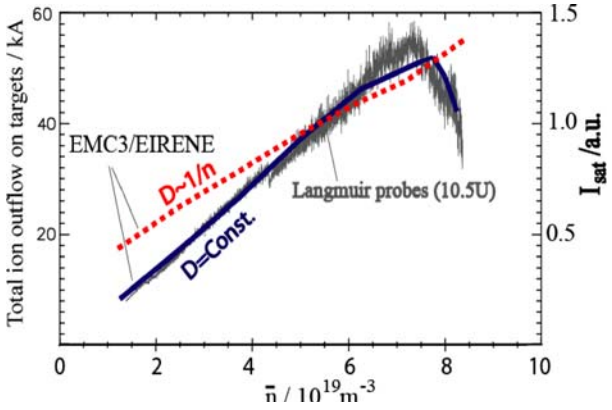

Fig. 4 Ion saturation currents increase linearly with plasma density. This linear-dependence can well be reproduced by the 3D code, independent on the D-ansatz.

poloidal and radial directions [9], while in LHD the radial approach of counter-flows residing on neighboring island chains is the main reason for flow damping [8,10]. As a consequence, a high recycling regime as observed in tokamaks does not take place in the island/stochastic SOLs of W7-AS and LHD and is also not expected by modeling. As an example for LHD, figure 4 shows a typical density dependence of the ion saturation currents measured by target Langmuir probes. In consistence with H_a-signals, I_{sat} grows linearly with increasing the line average density up to a rollover point. This linear behavior can be well reproduced by the EMC3/EIRENE code, insensitive to the selected D-ansatz. Nevertheless, the use of a constant D results in an ion flow slope matching better that of I_{sat} from the probes.

The larger field line pitch in W7-X decreases the perpendicular-to-parallel transport ratio, generally reducing the perpendicular viscous transport. Moreover, the large poloidal extension of the W7-X islands avoids cross-field frictional momentum interaction between adjacent island fans. This suggests that the SOL transport in W7-X should behave differently from that in W7-AS and LHD. This is indeed shown by EMC3/EIRENE simulations [16], as demonstrated in figures 5 and 6, where the W7-AS simulations serve as references. Simulations are carried out for pure hydrogen plasmas without impurities, for the respective standard ID configurations based on vacuum field. The SOL power for W7-AS is taken to be 1 MW which is up-scaled with the area of the LCFS to 10 MW for W7-X. The cross-field transport coefficients are set as D = 1 m^2/s and $\chi_i=\chi_e=3\times D$ which hold for both devices. At low plasma separatrix density n_{es} – the average density on the LCFS, both devices show linear growths of the recycling flux Γ_{recy} and the downstream density n_{ed} with increasing n_{es} up to ~1.3×10^{19} m^{-3}. Then, the W7-X results suddenly depart from the linear behaviour further followed by W7-AS. In this range, n_{ed} in W7-X approaches a scaling of $n_{ed} \sim n_{es}^3$ and greatly exceeds n_{es}, as it usually behaves in a high recycling regime found in tokamaks. W7-X is the first helical device for which a high recycling regime is predicted not only by the 3D code but also by 2D approximations [17]

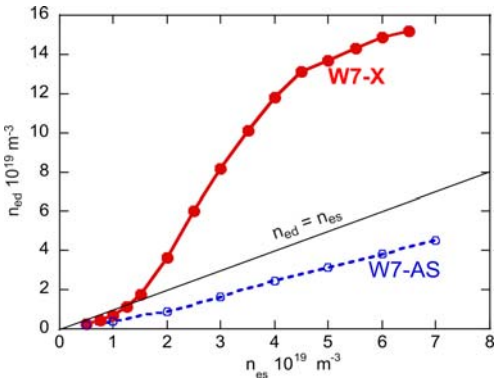

Fig.5: Comparison of n_{es}-dependences of the downstream density n_{ed} between W7-AS and W7-X.

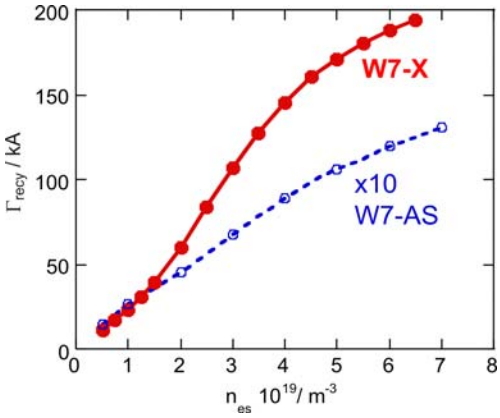

Fig.6: Responses of the total recycling flux Γ_{recy} to the spepatrix density n_{es} predicted for the respective W7-AS and W7-X standard island divertors.

5. Divertor function on reducing impurity influx

Reducing the impurity release from plasma facing components and preventing impurities from transporting towards the confinement plasma belong to the main design objectives of a divertor. Related theoretical research made for W7-AS so far was concentrated on exploring favorable divertor plasma conditions for reducing the impurity influx, mainly based on EMC3/EIRENE modeling started after the shutdown of W7-AS in 2002. Thus, iterations between theory and experiment have become hardly possible, leaving open theoretical issues

for further experimental confirmations. Fortunately, the work can be continued in LHD - the only helical device presently operated with divertors. This paper addresses only the numerical examinations and assessments of some essential factors affecting the impurity influx. Related experimental studies and results are referred to in Refs [18, 19].

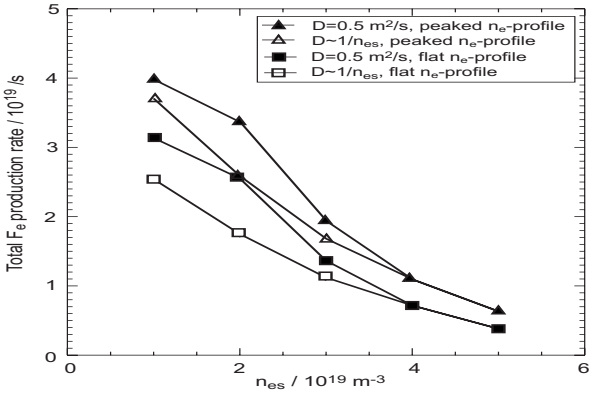

Fig.7 Sensitivities of high-energetic CX-neutrals to core profiles and cross-field transport coefficients as well as separatrix density, calculated by ECM3-EIRENE for W7-AS.

5.1 Impurity source

Both the ID in W7-AS and the HD in LHD have an open divertor structure and the first wall is made of stainless steel. High-energetic CX-neutrals hitting the wall are a potential source of impurities by means of physical sputtering. An optically-thick island/stochastic SOL can move the CX-neutrals to a lower energy band in the energy spectrum and thereby reduce the sputtering-relevant neutral flux. For a given input power entering the SOL, the SOL temperature drops with increasing the SOL density, especially at the downstream of maximum population of the recycling neutrals. Figures 7 and 8 show respectively the density dependences of the total Fe yield sputtered by CX-neutrals for W7-AS [20] and LHD. Because of the existing uncertainties in wall conditioning, the Fe yield shown here should be regarded as a physics quantity for measuring the sputtering-relevant, high-energetic CX-neutral flux. For both W7-AS and LHD, the 3D code simulation results show that a dense, cold island/stochastic SOL can effectively reduce the high-energetic CX-neutral flux and thereby the sputtered Fe yield.

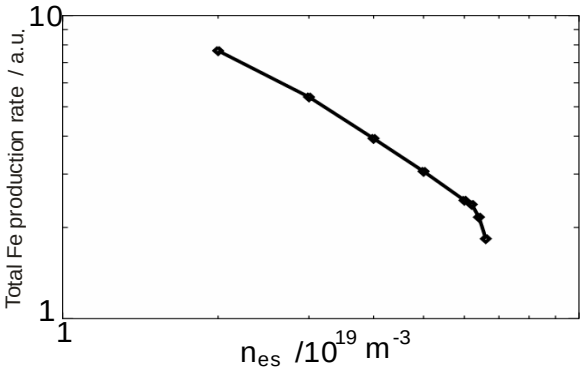

Fig.8 Calculated Fe-prodution rate as a function of n_{es} in LHD.

5.2 Impurity SOL transport

High-Z impurities like the wall-released Fe impurities can, even with a reduced source, cause significant radiation loss and contamination if they reach the confinement core region, preventing plasma from a high density operation. Impurity transport in the complex 3D SOLs of the W7-AS ID and the LHD HD has been studied using EMC3/EIRENE code based on trace impurity model. The divertor-released carbon is used as a representative impurity species. There are good reasons to do this. First, the parallel impurity flow velocities induced by

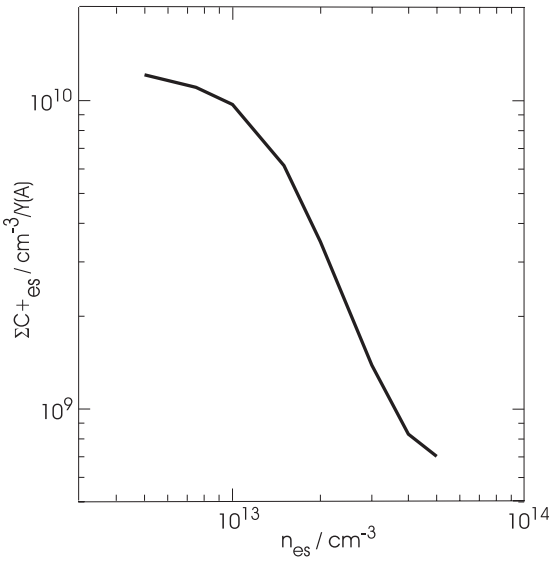

Fig. 9: Carbon separatrix density as a function of n_{es} from 3D simulations.

the dominating friction and ion thermal forces are largely independent of the charge and mass of the impurity species. Second, the multiple island structures in both machines distribute the background plasma flows over almost the whole SOL periphery in both poloidal and toroidal directions. Thus, the whole SOL periphery has the meaning of downstream. Third, edge carbon spectroscopic measurements are available at LHD. Carbon neutrals are started from the targets with an initial energy of 0.1 eV, resulting in a penetration depth comparable with that of physically-sputtered Fe-impurities with a sputtered energy of several eV. With a fixed carbon source strength, the plasma density is varied in order to check the carbon transport behavior under different SOL plasma conditions. The results for W7-AS are shown in figure 9 [11]. One sees a sharp drop of the carbon separatrix density with increasing the plasma density in the range from 1 to 3×10^{13} cm^{-3}, meaning that a dense SOL plasma has a retention effect on the carbon impurities. Similar effect has been also predicted for the stochastic layer in LHD [12]. Figure 10 shows how the carbon density profiles through the stochastic layer in the LHD HD change from peaked to hollow with increasing the plasma separatrix density. Parallel-force balance analysis based on the 3D simulations shows that the net force acting on impurities can, with increasing the SOL density, be changed from thermal-force dominated to friction dominated, leading to a reversal of the convective impurity flow from inwards- to outwards-directed. This is the reason for the reduced carbon density at the inner separatrix under high density conditions.

The island screening potential on intrinsic impurities is also examined for the standard ID of W7-X [16]. Using the calculated background plasmas shown in figures 5 and 6, test carbon impurities are sampled on the targets following the deposition profiles of the background ions calculated by the EMC3 code for individual cases. With a fixed total sputtered flux of $1/1.6\times10^{-19}$ particles/s, carbon atoms are started with mono-energies of E_0 = 0.1, 1 and 10 eV, respectively, covering both chemical and physical sputtering processes. Figure 11 shows the dependences of the averaged carbon density at the inner separatrix, n_{cs}, on n_{es} and E_0. In all the selected E_0-cases, n_{cs} drops sharply in the n_{es}-range from 1 to 2×10^{19} m^{-3}. A lower n_{es}–boundary is set at 1×10^{19} m^{-3} in figure 11 to cut off the low SOL collisionality cases where $\lambda_{i,e}/L_c < 10$. The strong drop in n_{cs} is associated with a transition from thermal-force to friction-dominated impurity transport in the SOL, as understood from W7-AS and LHD. This transition is sharper in W7-X because of the high recycling regime. Higher-energetic carbon neutrals penetrate more deeply into the SOL, causing an overall increase in n_{cs}. This means that the islands have a less screening efficiency on high-energetic impurities than on low-energetic ones, as expected. Nevertheless, the n_{es}-dependences are largely independent of E_0, indicating that the SOL density is always a sensitive tuning parameter for controlling the influxes of both the chemically and physically sputtered impurities.

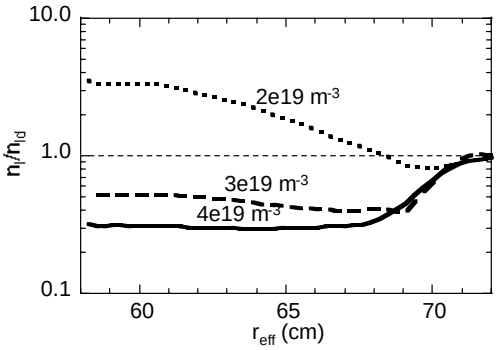

Fig.10: Radial profiles of total carbon density n_I normalized by downstream density n_{Id} in ergodic layer of LHD for different background plasma densities, obtained from 3D modelling.

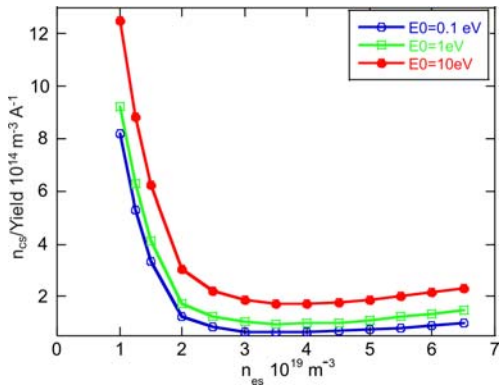

Fig. 11: Sensitivities of carbon density at the inner separatrix, n_{cs}, to n_{es} and initial energy of the sputtered carbon atoms, E_0. n_{cs} is normalized to a total carbon production rate of $1/1.6\times10^{-19}$ s^{-1}.

6. Summary

The island divertor tested at W7-AS and followed by W7-X and the helical divertor presently operated at LHD have a common geometric feature, i.e. that the low-order magnetic islands are the basic elements forming the divertor SOLs, laying a basis for a reasonable comparative divertor transport study. EMC3/EIRENE simulations in comparison with Thomson-scattering measurements have revealed the fundamental role of the low-order magnetic islands for plasma transport in the stochastic layer of LHD. Parallel plasma flows are modulated by the specific island structures in individual devices. Viscous-transport induced momentum loss due to topological approaches of opposite flows residing on adjacent island fans is considered to be the reason for the absence of a high recycling regime in W7-AS and LHD. The larger islands in W7-X avoid the viscous interaction between opposite flows. As a consequence, a high recycling regime is expected to take place in W7-X from both 2D and 3D simulations. Regarding the divertor function on reducing the impurity influx, EMC3/EIRENE simulations show that a dense SOL plasma can significantly reduce the wall impurity release induced by the CX-neutrals escaping from the open divertors in both W7-AS and LHD. Moreover, the 3D code demonstrates that, under high SOL collisionalities, the edge magnetic islands in all the three devices have a similar screening effect on intrinsic impurities. This happens when the cross-field heat conduction governs the ion energy transport across the islands under high density, low temperature conditions. In this case, the friction force dominates over the ion thermal force, dragging impurities outwards.

References

[1] R. König *et al., PPCF* **44**, 2365 (2002)
[2] P. Grigull *et al., PPCF* **43**, A175 (2001)
[3] H. Renner *et al., Nucl. Fusion* **40**, 1083 (2000)
[4] N. Ohyabu *et al., Nucl. Fusion* **34**, 387 (1994)
[5] Y. Feng *et al., J. Nucl. Mat.* **266-269**, 812 (1999)
[6] D. Reiter, *Fusion Sci. Technol.* **47**, 172-86 (2005)
[7] J. Miyazawa *et al., Nucl. Fusion* **46,** 532 (2006)
[8] M. Kobayashi *et al., J. Nucl. Mater.* **363-365** 294 (2007)
[9] Y. Feng *et al., Nucl. Fusion* **46**, 807 (2006)
[10] Y. Feng *et al., Nucl. Fusion* **48**, 024012 (2008)
[11] Y. Feng *et al., 32nd EPS,* vol **29C** (ECA), P1.012 (2005)
[12] M. Kobayashi *et al., Contrib. Plasma Phys.* **48**, 255 (2008)
[13] R. Brakel *et al., "Improved performance of the W7-AS stellarator with the new island divertor", 19th IAEA Fusion Energy Conference, Lyon, France,* 2002, IAEA-CN-94/EX/C5-4
[14] Y. Nakamura *et al., Nucl. Fusion* **43**, 219 (2003)
[15] M. Kobayashi *et al., "Model prediction of impurity retention in ergodic layer and comparison with edge carbon emission in LHD", 18th inter. Conference on Plasma-Surface Interactions in Controlled Fusion Devices, Toledo, Spain,* 2008, O-3
[16] Y. Feng *et al.,"EMC3/EIRENE Transport Modelling of the Island Divertor in W7-X",35th EPS, Hersonissos, Crete, Greece, 2008, P2.085*
[17] J. Kisslinger *et al.,* EPS 19C, II, 149 (1995)
[18] R. Buhrenn et al., this conference
[19] M. Kobayashi *et al.*, this conference
[20] Y. Feng *et al., J. Nucl. Mater.,* **363-365** (2007) 353